

# One-dimensional growth of rock-salt PbS nanocrystals mediated by surfactant/polymer templates\*

Shihe Yang<sup>1†</sup>, Suhua Wang<sup>1</sup>, and K. K. Fung<sup>2</sup>

*Department of Chemistry<sup>1</sup> and Department of Physics<sup>2</sup>, Hong Kong University of Science and Technology, Clear Water Bay, Kowloon, Hong Kong*

*Abstract:* A novel method has been developed for the synthesis of compound semiconductor nanorods (PbS). This method consists of using a functionalized lead(II) salt  $\text{Pb}(\text{AOT})_2$  as the precursor and a polymer (PVB) as both a matrix and a stabilizer. The PbS nanocrystallites prepared using this method are all oriented with their (100) lattice planes parallel to the substrate surface. Possible mechanisms are briefly discussed for the growth of the rod-shaped PbS nanocrystals with the preferred orientation in the polymer film.

## INTRODUCTION

One-dimensional semiconductor nanoclusters have some special characteristics due to their large surface-to-volume ratio, quantum size effect, and dielectric confinement effect [1–6]. They are expected to exhibit a variety of new spectroscopic features, including sharper absorption spectra, enhanced exciton and impurity binding energies, and modified electron–phonon coupling. Semiconductor nanowires may be used to inter-connect nanodevices as electronic components become ever smaller due to incessant miniaturization. Their unique electronic, magnetic, and optoelectronic properties allow themselves to function as nanodevices in information processing and storage. Moreover, they can be used as nano-probes to the nano-world as nanotechnology really becomes the workforce of the 21<sup>st</sup> century.

Growth of one-dimensional nanostructures has traditionally been associated with such highly technological processes as vapor deposition, lithography, STM, and AFM [7,8]. Chemical synthesis may become the method of choice for fabricating metal and semiconductor nanowires under mild conditions [9,10]. It has long been established that surfactant molecules can self-assemble to form many ordered structures at different levels and at nanometer scale [11,12]. By taking advantage of these fascinating structures, one could design different nanoscale quantum devices. This templating route appears to be more advantageous than the brute-force approach to arrest metastable low-dimensional nanostructures. The template itself is created by thermodynamic driving forces, but the metastable nanostructures can only be produced through kinetic constraints in the templated reactions. Using a copolymer ionomer template, we have recently synthesized PbS quantum dots [13]. The goal of the present work is to explore the growth protocol for one-dimensional PbS semiconductor nanocrystals using a surfactant/polymer template.

## SYNTHETIC METHOD

Details on the PbS nanorod synthesis have been given elsewhere [14]. Here we only provide a brief description. Figure 1 illustrates the strategy we used to synthesize PbS nanorods in a poly(vinyl butyral)

---

\**Pure Appl. Chem.* **72**, 1–331 (2000). An issue of reviews and research papers based on lectures presented at the 1<sup>st</sup> IUPAC Workshop on Advanced Materials (WAM1), Hong Kong, July 1999, on the theme of nanostructured systems.

<sup>†</sup>Corresponding author: E-mail: chsyang@ust.hk

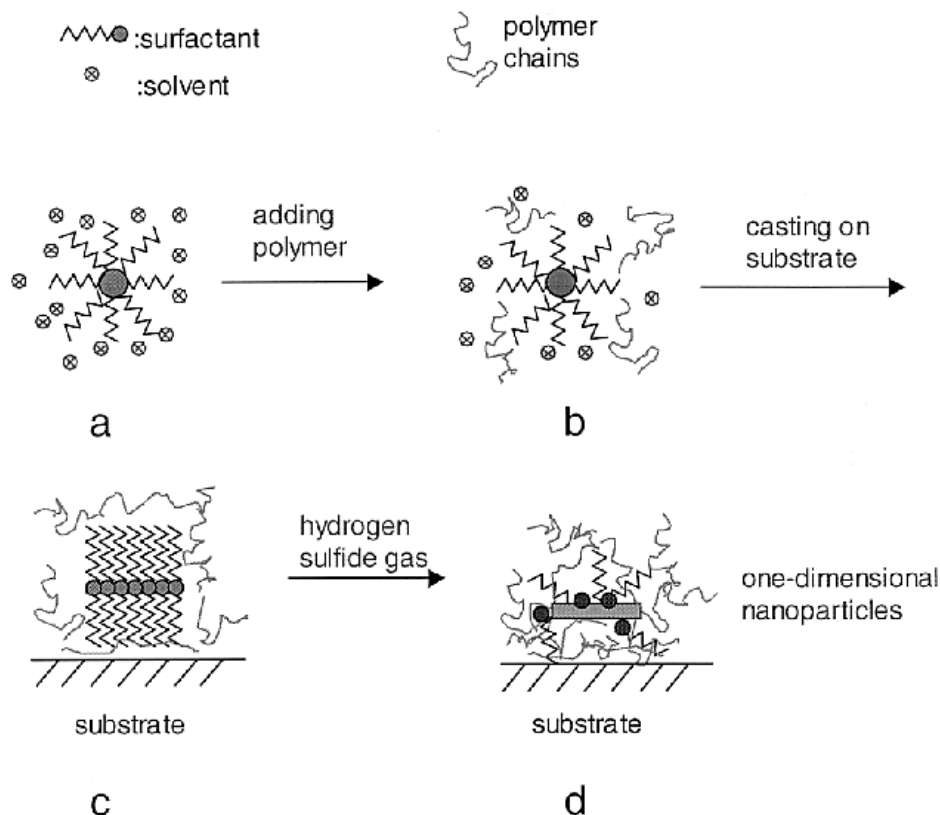


**Fig. 1** A schematic illustration of the strategies for the synthesis of PbS nanorods in PVB film.

(PVB) film. We started with a reversed micelle ( $\text{Pb}(\text{AOT})_2$ ) in a chloroform solution (Fig. 1a). After introduction of PVB molecules, the micelles were stabilized by attaching the PVB molecules to the micelle surfaces (Fig. 1b). When the micelle solution was dip cast on a glass slide, structural rearrangement occurred due to mechanical shear and rapid evaporation of solvents, resulting in a lamella structure (Fig. 1c). The lamella domain was used as a pre-defined precursor structure for the PbS nanocluster growth. This precursor appears to be stabilized and protected by the polymer entanglement. The semiconductor nanostructures were then created by gas–solid reaction (Fig. 1d). The nanostructures thus created may be of zero-, one-, and two-dimensions depending on the experimental conditions. Due to the polymer matrix, dynamic exchange of the surfactants was hindered. In an actual experiment, the procedure is as follows: first, the  $\text{Pb}^{2+}$  ions were exchanged into the ionic surfactant to form  $\text{Pb}(\text{AOT})_2$ . The ion-exchanged surfactant formed micelles in the solution. PVB was added to the solution to protect the micelle structures. The surfactant/polymer solution was then cast on a glass substrate as a uniform film. Lastly,  $\text{H}_2\text{S}$  gas was infused into the polymer film to form a PbS/AOT/PVB nanocomposite.

### LATTICE PLANE ORIENTATIONS OF PBS NANOCRYSTALS

Figure 2 shows the XRD patterns of the PbS nanocrystals prepared in the PVB film with different Pb/PVB ratios (traces a and b). The XRD pattern of a PbS powder is also shown in Fig. 2 (trace c) for comparison. First of all, the diffraction peaks of the nanocrystals have a one-to-one correspondence to

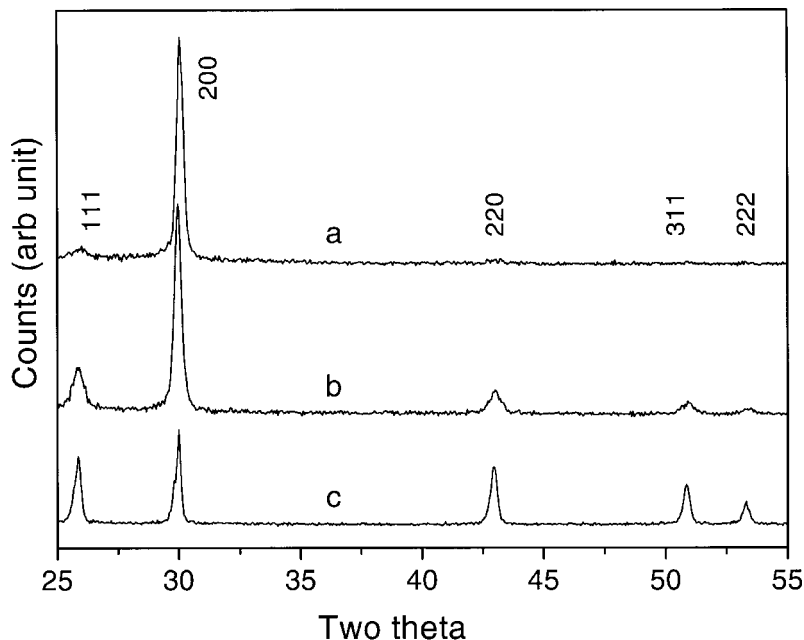


**Fig. 2** XRD patterns of PbS nanocrystals with the molar ratios of Pb(II)/PVB being 12.0 (trace a) and 9.72 (trace b), respectively. Trace c displays a XRD pattern of a powder PbS sample for comparison.

those of the PbS powder, confirming the formation of fcc PbS nanocrystals. Secondly, it is clearly recognized that the (200) diffraction peak of the nanocrystals is much stronger than that of the powder PbS. In other words, the intensity distribution of all the observed X-ray diffraction peaks of the nanocrystals deviates drastically from the characteristic pattern of bulk PbS (galena) powders. It appears that the PbS nanocrystals dispersed in the PVB film are oriented in such a way that their (100) planes are parallel to the substrate surface. In passing, highly oriented triangular PbS crystals were reported using the Langmuir–Blodgett technique [15].

Another observation from Fig. 2 is that the intensity distribution of the diffraction peaks depends on the concentration ratio Pb/PVB used to prepare the nanocrystals. For example, the intensity ratio ( $I_{200}/I_{111}$ ) of the first two peaks in the XRD pattern increases with increasing Pb/PVB ratio. A large intensity ratio ( $I_{200}/I_{111}$ ) is correlated to a high degree of orientation of the (100) lattice plane and vice versa. The above result therefore demonstrates that the (100) lattice planes of the PbS nanorods prepared in the PVB polymer film become better oriented as the concentration of  $\text{Pb}(\text{AOT})_2$  increases. For samples with sufficiently high Pb(II) concentrations, the intensity of the (111) diffraction peak was too weak to be measured accurately. In other words, all the PbS nanorods were orientated with their (100) planes parallel to the substrate surface given a sufficiently high Pb(II) concentration. On the other hand, for samples with too low Pb(II) concentrations, the intensity of all the diffraction peaks was too weak to be determined accurately.

### ONE-DIMENSIONAL STRUCTURE OF PbS NANOCRYSTALS

A typical TEM image of the PbS samples prepared in the PVB film is shown in Fig. 3. It is striking that essentially all the PbS species are of the rod shape on this magnification scale. These PbS rods were formed at room temperature with the ratio of  $\text{Pb}(\text{AOT})_2/\text{PVB}$  being  $3.34 \times 10^{-4}$  mol/g and the  $\text{H}_2\text{S}$  gas

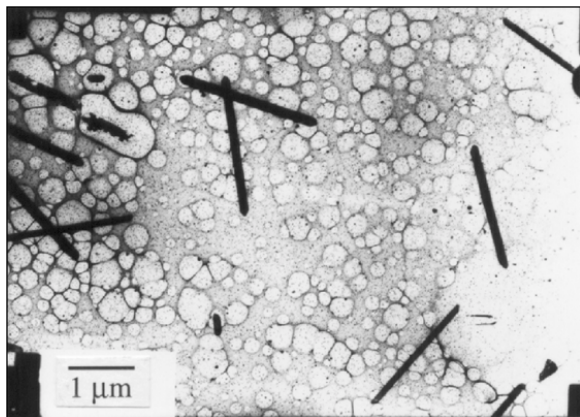


**Fig. 3** TEM image of the PbS nanorods formed in PVB polymer film.

exposure time being 12 h. Although some much smaller PbS particles (3–5 nm) with roughly spherical shape are also present in the TEM image, it is clear that their volume is small compared with that of the rods. Moreover, we believe that at least some of these ultrafine particles might be formed during the TEM sample preparation. Because the PbS rods were trapped in the PVB polymer, they are difficult to image directly using TEM. We therefore used chloroform to dissolve the polymer matrix. The bubble-like features seen in the TEM image shown in Fig. 3 are the chloroform-induced polymer/surfactant assemblies.

Under appropriate conditions ( $5 \times 10^{-6}$  M PbS/ $\text{CHCl}_3$ , rapid solvent evaporation), the bubbles could be arranged into a well-defined hexagon network as shown in Fig. 4a. In this hexagon network, only very small nanocrystals (a few nm in diameter) of irregular shape were observed. Fig. 4b shows a typical HRTEM image of the PbS nanocrystals in the hexagon network with fringe spacing corresponding to those of (111) and (200) lattice planes. It appears that during this dissolution process, the PbS nanorods may have suffered from severe strain which led to fracture and breakage to smaller particles with irregular shapes. This is also supported by XRD measurements (see Fig. 5). As shown in Fig. 5a, the XRD pattern shows a strong (200) diffraction peak characteristic of the preferential orientation of the (100) lattice plane. However, the XRD pattern changed to essentially a powder pattern (Fig. 5b) after the solvent dissolution. Because the thinner and longer rods are more likely to be broken, the

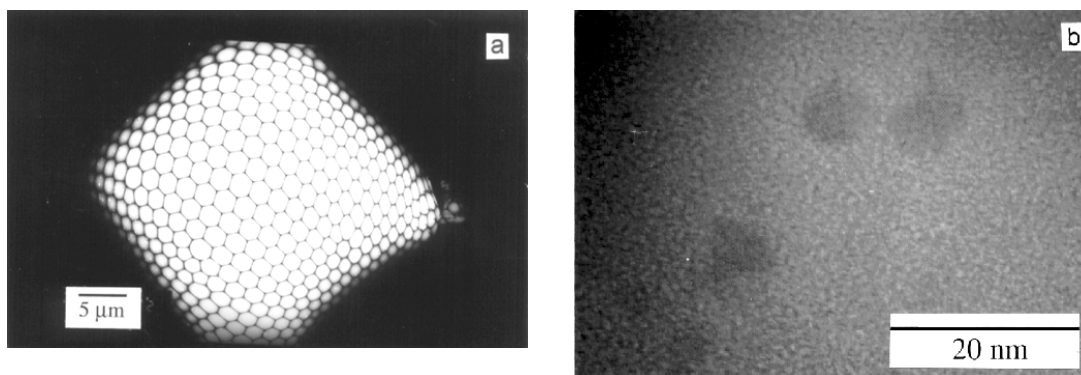


**Fig. 4** (a) Electron micrograph of PbS/AOT/PVB hexagon network. (b) HRTEM image of PbS nanocrystals after solvent dissolution.

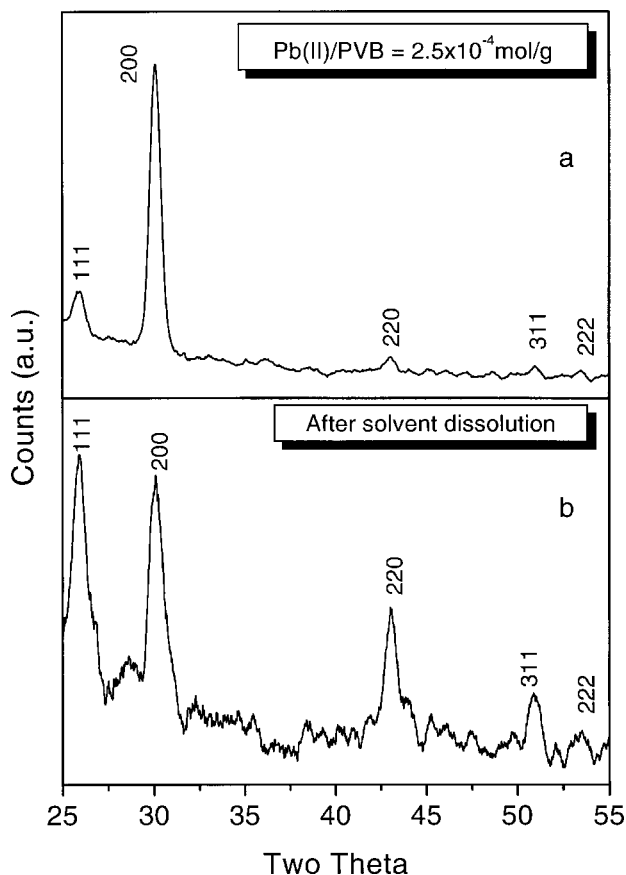


**Fig. 5** XRD patterns of (a) PbS nanorods prepared in PVB film, (b) PbS nanocrystals after solvent dissolution.

actual average aspect ratio of the PbS nanorods in the polymer film may be much larger than that estimated from the TEM image in Fig. 2.

High-resolution TEM images of PbS nanorods have also been obtained. Well-defined fringes were revealed, running all the way along the rod direction. The fact that the fringe pattern can be resolved by TEM indicates that the PbS rods are somewhat thinner than the width. Therefore, these one-dimensional PbS nanocrystals should be more correctly called PbS nano-strips. The fringe spacing is estimated to be 0.287 nm, which is close to the (200) lattice spacing of PbS. As was shown by electron diffraction and by XRD, the (200) lattice planes of the PbS nanorods are oriented parallel to the substrate, which suggests that the preferred particle growth is in the (200) direction. This growth pattern was observed by Weller et al. for PbS needles in amphiphilic block copolymer micelles [16].

It was found that not only the average particle size, but also the average aspect ratio (the ratio of length to width) of the PbS nanorods as affected by the lead(II) concentration and the detailed preparation procedures. When the PbS nanorods were formed with the molar ratio of Pb(II)/PVB being 12.0, they have a relatively large aspect ratio and a narrow size distribution. The PbS rods are  $2.2 \pm 0.2 \mu\text{m}$  in length and  $105 \pm 30 \text{ nm}$  in width. The average aspect ratio is  $\sim 20$ . Experimental results revealed that the necessary concentration for forming PbS rods is within a narrow range of the Pb(II)/PVB molar ratios, 7.6 ~ 35. Only disk-like particles were formed if the concentration of Pb(AOT)<sub>2</sub> is beyond the range. Moreover, the change in the aspect ratios of the PbS nanorods within the narrow concentration range was found to be gradual.

### GROWTH MECHANISM OF ORIENTED PBS NANORODS

We have followed the growth of PbS nanocrystals after termination of H<sub>2</sub>S exposure using UV-vis spectroscopy. The UV-vis absorption spectra of the PbS nanocrystals prepared in PVB film are shown in Fig. 6a. Clearly, the spectra display a dramatic deviation (blue-shift) from that of the bulk PbS. The UV-vis absorption of the PbS nanorods starts at ~800 nm and increases smoothly with decreasing wavelength, giving rise to a featureless spectrum. The UV-vis absorption spectra as a function of the time after H<sub>2</sub>S exposure (Fig. 6a) demonstrate the stability of the nanocrystals against aggregation for the PbS nanorods prepared in PVB film. For the film-gas reaction, the particle size was affected only by the H<sub>2</sub>S exposure time. When the H<sub>2</sub>S exposure time was lengthened, the absorption edge shifted to longer wavelength, indicating the continuous growth of the PbS nanorods. However, when the films were removed from the H<sub>2</sub>S atmosphere, no further red shift took place in the absorption spectra and the spectra did not change much with time. This is attributed to the restricted motion of the molecules in the polymer film, and therefore the limited change in surface states.

Shown in Fig. 6b are the corresponding UV-vis spectra of the nanocrystals prepared in solution with the same Pb/PVB ratio as in the film synthesis. When the solution was removed from the H<sub>2</sub>S atmosphere, the absorption edge kept on shifting to longer wavelengths with the elapse of time. This indicates that the aggregation of existing small particles might be an important process to form large particles in the solution phase. This is understandable because small particles are in constant motion,

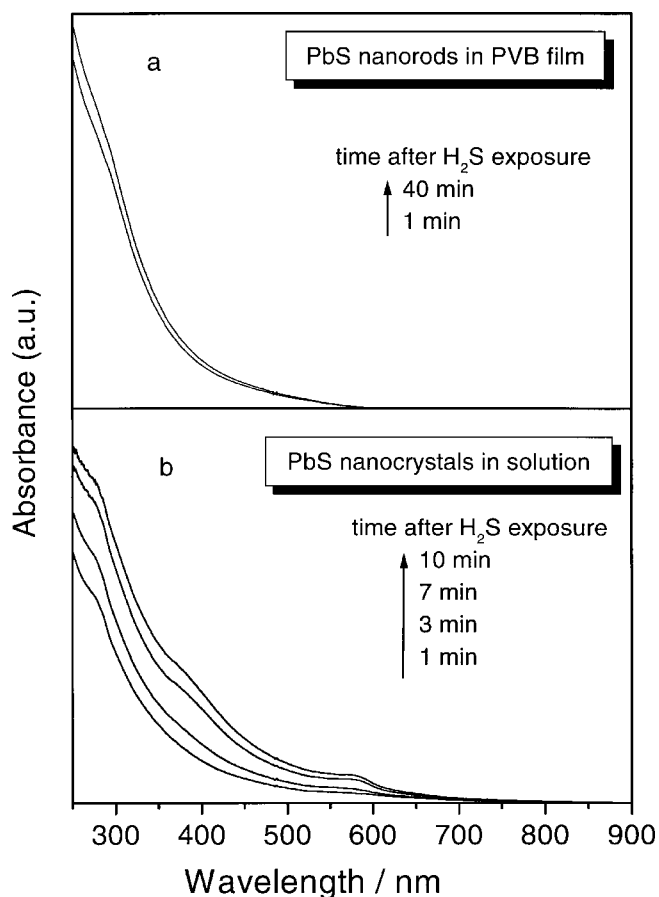


**Fig. 6** UV-vis spectra of the PbS nanocrystals synthesized in PVB film (a) and in solution (b). The spectra were taken after termination of H<sub>2</sub>S exposure. Shown on the right of the arrows are time elapses after termination of H<sub>2</sub>S exposure.

and when they encounter each other, aggregation or coalescence may take place if their capping molecules can undergo dynamic exchange with molecules in solution. With the elapse of time, the spectra of the PbS nanocrystals evolve eventually to a spectrum which has an absorption onset of 750 nm with three salient shoulders around 600 nm, 400 nm, and 300 nm. These three shoulders are due to exciton absorptions, which were attributed to  $1s_e-1s_h$ ,  $1s_e-1p_h$ , and  $1p_e-1p_h$  transitions, respectively [17]. One of the reasons for the absence of exciton absorption peaks in the spectra of PbS nanorods (Fig. 6a) is that the nanorods are confined only in two directions and the third dimension is extended. This may wash out the exciton absorption peaks. In fact, even the width of the PbS nanorods are much larger than the Bohr radius of bulk PbS. An alternative explanation is related to the surface structure of the nanoparticles [18,19]. The appearance of these three peaks implies that the excitons are not or less perturbed by the surface-trapped electron-hole pairs. In the solution synthesis, as the PbS nanoparticles grow, AOT<sup>-</sup> may diffuse away, leaving the HO- groups of PVB to be attached to the nanoparticle surface [20]. It follows that the exciton peaks are observed as in PVA-capped PbS nanoparticles. However, in the polymer film, the diffusion of AOT<sup>-</sup> is hindered, and its  $-SO_3^-$  groups may stick to the PbS nanoparticle surface. The strong electron-hole trapping effect of the ionic group may also render the exciton absorption peaks unobservable.

The results presented above showed that PbS can be grown into one-dimensional rods with a preferred (100) orientation parallel to the substrate surface. The question as to why such a highly symmetric cubic crystal can grow in one dimension with a large aspect ratio points directly to the role of Pb(AOT)<sub>2</sub>/PVB as a precursor, which is crucial in growing the nanorods and defining the crystal plane orientations (Fig. 1). During the process of transferring the micelle solution onto a glass substrate by dip casting, a lamella structure was formed. Each lamella domain was stabilized by interactions with the PVB polymer chains through van der Waals forces and hydrophobic effects [21].

Evidence for the lamella structure on the glass substrate is provided by the XRD pattern of the film. No diffraction peaks were observed in the XRD pattern of pure PVB film. It is only when the PVB was loaded with Pb(AOT)<sub>2</sub> that diffraction peaks started to appear. These diffraction peaks are ascribable to a lamella structure of Pb(AOT)<sub>2</sub> in the PVB film. Furthermore, the Pb(AOT)<sub>2</sub>/PVB multilayers exhibit a nearest inter-plane distance of  $\sim 22.0$  Å as calculated from the series of diffraction peaks. In this layered structure, Pb(II) ions are arranged in two-dimension parallel to the substrate. As the H<sub>2</sub>S molecules diffused into the layered structure, they reacted with the Pb(II) ions to produce PbS nanoclusters with the original Pb(II) planes being developed into the (100) lattice plane of the PbS nanorods. In addition, the diffusion of H<sub>2</sub>S into the hydrophilic domain and the formation of the PbS nucleation center are bound to modify the original layered structure. A likelihood is that a curvature develops and the layered structure curls up, starting to form one-dimension structures. The growth of PbS then proceeds in one dimension. This is supported by the disappearance of the original diffraction peaks after exposure to the H<sub>2</sub>S gas.

It is believed that the curvature of the layered structure restricts the lateral growth of the PbS nanocrystals, whereas the amount of the Pb(II) in each domain determines their thickness. When the Pb(II)/PVB ratio is too low, each domain may be too small to form even the layered precursor structure as shown by the XRD data. On the other hand, when the Pb(II)/PVB ratio is too high, each domain would be too large to curl up effectively. In this situation, the diffusion of H<sub>2</sub>S and the formation of the PbS nucleation center simply destroyed the layered structure, forming spherical particles. However, the orientation of the (100) plane is still preserved in the initial nucleation stage.

## CONCLUDING REMARKS

We have developed a synthetic route for growing novel one-dimensional PbS nanocrystals (nanorods) using a combination of surfactant and polymer matrix as the template. These nanocrystals have a preferred

(100) lattice plane orientation parallel to the substrate surface. We have investigated some important experimental parameters which can be used to control the PbS nanocrystal size, shape, surface states, and crystal plane orientation. These nanoclusters have a relatively large aspect ratio and most of them have a preferred crystal plane orientation relative to the substrate surface. For comparison, solution preparation of PbS nanocrystals was carried out under similar conditions, and only spherical particles were obtained. This provided some clue for understanding the mechanism of the PbS nanorod growth in the PVB films. Given the generality of this approach, we hope to extend our synthetic method to the preparation of other one-dimensional semiconductor nano-sized materials with preferential crystallite plane orientations.

#### ACKNOWLEDGMENT

This work is supported by an RGC grant administered by the UGC of Hong Kong.

#### REFERENCES

1. J. Voit. *Rep. Prog. Phys.* **58**, 977–1116 (1994).
2. *Highly Conducting One-Dimensional Solids* (J. T. Devreese, R. P. Evrard, V. E. van Doren, eds.), Plenum, New York (1979).
3. C. M. Lieber and X. L. Wu. *Acc. Chem. Res.* **24**, 170–177 (1991).
4. H. Dai and C. M. Lieber. *Annu. Rev. Phys. Chem.* **44**, 237–263 (1993).
5. C. M. Lieber, J. Liu, P. E. Sheehan. *Angew. Chem. Int. Ed. Engl.* **35**, 687–704 (1996).
6. J. Hu, T. W. Odom, C. M. Lieber. *Acc. Chem. Res.* **32**, 435–445 (1999).
7. H. Namatsu, K. Kurihara, M. Nagase, T. Makino. *Appl. Phys. Lett.* **70**, 619–621 (1997).
8. J. Wang, D. A. Thompson, B. J. Robinson, J. G. Simmons. *J. Cryst. Growth* **175**, 793–798 (1997).
9. M. P. Pileni, T. Gulik-Krzywicki, J. Tanori, A. Filankembo, J. C. Dedieu. *Langmuir* **14**, 7359–7363 (1998).
10. W. Q. Han, S. S. Fan, Q. Q. Li, Y. D. Hu. *Science* **277**, 1287–1289 (1997).
11. M. Antonietti and C. Goltner. *Angew. Chem. Int. Ed. Engl.* **36**, 910–928 (1997).
12. *Biomimetic Materials Chemistry* (S. Mann, ed.), VCH, New York (1996).
13. Z. H. Zeng, S. H. Wang, S. H. Yang. *Chem. Mater.* **11**, 3365–3369 (1999).
14. S. H. Wang and S. H. Yang. *Langmuir* **16**, 389–397 (2000).
15. X. K. Zhao, J. Yang, L. D. McCormick, J. H. Fendler. *J. Phys. Chem.* **96**, 9933–9939 (1992).
16. T. Schneider, M. Haase, A. Kornowski, S. Nased, H. Weller. *Ber. Bunsenger Phys. Chem.* **101**, 1654–1656 (1997).
17. J. L. Machol, F. W. Wise, R. C. Patel, D. B. Tanner. *Phys. Rev. B* **48**, 2819–2822 (1993).
18. Y. Wang and N. Herron. *J. Phys. Chem.* **95**, 525–532 (1991).
19. M. Gao, Y. Yang, B. Yang, J. Shen, X. Ai. *J. Chem. Soc. Faraday Trans.* **91**, 4121–4125 (1995).
20. M. T. Nenadovic, M. I. Comor, V. Vasic, O. I. Micic. *J. Phys. Chem.* **94**, 6390–6396 (1990).
21. R. P. Andres, J. D. Bielefeld, J. I. Henderson, D. B. Janes, V. R. Kolagunta, C. P. Kubiak, W. J. Mahoney, R. G. Osifchin. *Science* **273**, 1690–1693 (1996).